

ENGINEERING THE MICROSTRUCTURE AND OPTICAL FEATURES OF SiC-MWCNTS NANOPARTICLES DOPED PVA-PAA FOR PROMISING INDUSTRIAL APPLICATIONS

UDC:66.017

Original scientific paper

<https://doi.org/10.46793/aeletters.2025.10.4.5>

Saad Abbas Jasim¹, Ali Mohammed Ali², Najah M. L. Al Maimuri³, Ahmed Hashim^{1*},
Mohammed H. Abbas¹

¹Department of Physics, University of Babylon, College of Education for Pure Sciences, Babylon, Iraq

²Department of Physics, College of Basic Education, University of Babylon, Iraq

³Building and Construction Technologies Engineering Department, College of Engineering and Engineering Technologies, Al-Mustaqbal University, 51001, Babylon, Iraq

Abstract:

The development of new materials with improved features requires the use of nanocomposite materials and polymer blends. Their special combination provides enhanced performance in a range of environmental, biomedical, and industrial applications. Using the traditional casting procedure, the polyvinyl alcohol (PVA) / poly acrylic acid (PAA) polymer blend doped with silicon carbide (SiC) / multi-walled carbon nanotubes (MWCNTs) nanocomposites was successfully created. Nanocomposites (NPs) were evenly distributed over the polymer mix matrix, and the polymer blend was well dispersed in the solution, according to the optical microscopy image. The films' surface morphology of the polymer blend exhibits a homogeneous grain distribution, according to FE-SEM examination. The generated materials do not include any new functional groups, according to the FTIR analysis, indicating that just a physical interaction has taken place. It was observed from the study of optical properties that the increase in SiC/MWCNTs nanoparticles led to enhancement of all optical features, such as absorbance, refractive index, optical conductivity, real and imaginary parts of the dielectric constant, while transmittance and energy gaps were decreased. The energy gap decreased from 4.8 eV to 3.82 eV for the allowed transition, and from 4 eV to 3.02 eV for the forbidden transition. These results reveal that PVA/PAA doped SiC/MWCNTs films can be utilized in a variety of advanced applications.

ARTICLE HISTORY

Received: 21 August 2025

Revised: 18 October 2025

Accepted: 26 November 2025

Published: 15 December 2025

KEYWORDS

PVA, Nanocomposites, PAA, Energy gap, SiC, MWCNTs, Absorbance, Blend

1. INTRODUCTION

Advanced materials known as polymer blend nanocomposites are created by blending two or more polymers together [1,2]. These materials are frequently reinforced with nanoscale fillers (1–50 nm), such as metal oxide nanoparticles, carbon nanotubes, graphene, or clay platelets, to produce multifunctional composites with improved

qualities. These blends take advantage of the specific blending of several polymer matrices [such as polyvinyl alcohol (PVA)/polyethylene glycol (PEG), polyacrylic acid (PAA), and polyethylene oxide (PEO)-based systems to balance conductivity, mechanical toughness, thermal stability, or biodegradability [3,4].

The majority of polymer blends are immiscible, necessitating compatibilization techniques to

*CONTACT: Ahmed Hashim, e-mail: ahmed.taay@yahoo.com

stabilize interfaces and avoid phase separation, either by reactive in situ polymerization or the addition of compatibilizer agents. Nanoscale fillers can significantly improve stiffness, tensile strength, barrier qualities, electrical or thermal conductivity, and even electromagnetic shielding when added to compatible blends because of their enormous interfacial area with the polymer [5,6].

PVA and PAA polymer blends exhibit a range of increased properties, making them extremely useful for biomedical and industrial applications [7]. Strong hydrogen bonds between the polymers greatly increase their mechanical strength; reports have shown up to 40-fold increases in toughness and tensile strength [8]. Additionally, these blends exhibit superior cytocompatibility and enhance cell adhesion, both of which are essential for tissue engineering, particularly cartilage repair. PVA/PAA hydrogels are perfect for drug delivery and smart material applications because they are pH-responsive and permit reversible swelling and shape changes [9]. With an adhesion force that increases by over 200% at physiological pH, they exhibit robust bio-adhesion [10]. A higher glass transition temperature in the blend indicates improved thermal stability, and the polymers exhibit good miscibility with a single, well-defined T_g [11]. Their swelling behavior stays constant in physiological settings, and their drug-release profile usually consists of a quick initial release followed by prolonged delivery [12]. PVA/PAA scaffolds' promise for cartilage tissue healing is confirmed by in vivo investigations that demonstrate their long-term maintenance of structural integrity and water content [13]. Overall, PVA/PAA blends are very adaptable for biomedical applications like scaffolds, wound dressings, and controlled-release systems due to their adjustable adhesion, swelling, and mechanical qualities [14].

SiC is a wide-bandgap semiconductor with an energy gap of approximately 3.0 to 3.3 eV, depending on the polytype, which enables excellent performance in high-temperature and high-power applications. Its optical features comprise strong absorption for UV and great thermal conductivity, making it appropriate for devices of optoelectronic and harsh environments. SiC also displays extraordinary chemical stability and mechanical hardness, making it ideal for use in power electronics, LEDs, and high-frequency devices. Recent developments focus on refining crystal growth methods and device production to improve their efficiency and reliability [15-20].

MWCNTs have special structural, electrical, and optical characteristics because they are made up of several concentric graphene cylinders [20]. Depending on their diameter and chirality, MWCNTs can have an adjustable bandgap that can be either metallic or semiconducting; they usually behave in a semi-metallic manner with a very small or nonexistent bandgap [21]. They are advantageous in photodetectors, sensors, and energy devices due to their great optical absorption over a broad spectrum, ranging from ultraviolet to near-infrared [22]. Applications in energy storage, composite materials, and nanoelectronics are made possible by their remarkable mechanical strength, electrical conductivity, and large surface area [23]. Current research focuses on improving their optoelectronic performance and customizing the band gap through doping and functionalization [24]. Adding both SiC and MWCNTs to polymer blends synergistically improves thermal conductivity, mechanical strength, and electrical properties, enabling advanced multifunctional composites. SiC contributes to enhanced heat dissipation, while MWCNTs offer superior reinforcement and electrical pathways [25]. There are several studies on structural, morphological, and optical properties of the advanced materials [26-29]. This study involves the fabrication of PVA/PAA/SiC/MWCNTs films and the examination of their optical, structural and morphological properties to be used in various advanced applications.

2. MATERIALS AND METHODS

The material used in the present work is a PVA/PAA polymer blend as a host matrix and SiC/MWCNTs as a filler. SiC (beta, 99 + %, < 80 nm, cubic) was obtained in nanopowder form from US Research Nanomaterials, Inc. MWCNTs were used as nanopowder with an outer diameter of 20-40 nm. A polymer blend consisting of 79 wt.% PVA and 21 wt.% PAA was prepared. Using a magnetic stirrer, both polymers were continuously dissolved in distilled water at 70°C until they were completely dissolved and a homogenous solution was produced. The polymer solution was then supplemented with SiC/MWCNTs hybrid nanoparticles at two distinct weight percentages: 0.6 wt% and 1.2 wt%. To guarantee that the nanoparticles were evenly distributed throughout the polymer matrix, the mixture was further agitated. The solution casting process was then used to pour the resultant mixture into sanitized Petri plates. To allow the solvent to completely

evaporate, the films were allowed to dry at room temperature for 7 days. The produced films were examined optically, structurally, and morphologically after they had dried. The experimental part is illustrated in Fig. 1. A micrometer was used to measure the films' thicknesses, which came out to be about 38 μm .

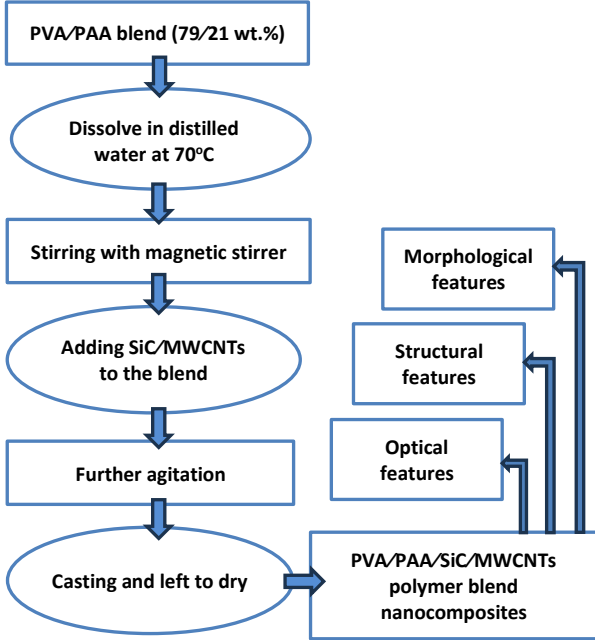


Fig. 1. Procedure of the experiment

The coefficient of absorption - α (cm^{-1}) is given by [30]:

$$\alpha = 2.303 \frac{A}{d} \quad (1)$$

where A - is the absorbance (AU) and d - is the thickness of films in (cm).

The energy gap is determined by the expression [31]:

$$(\alpha h\nu)^{\frac{1}{r}} = Y(h\nu - E_g) \quad (2)$$

where Y - is constant, $h\nu$ - is photon energy in (eV), E_g - is the energy gap in (eV), and r - is 2 and 3 for allowed and forbidden transitions. The refractive index n - is defined by [32]:

$$n = \frac{1 + \sqrt{R}}{1 - \sqrt{R}} \quad (3)$$

where R - is the reflectance. The extinction coefficient k - is given by [33]:

$$k = \frac{\alpha\lambda}{4\pi} \quad (4)$$

Real (ϵ_1) and imaginary (ϵ_2) parts of the dielectric constant are given by [34]:

$$\epsilon_1 = n^2 - k^2 \quad (5)$$

$$\epsilon_2 = 2nk \quad (6)$$

The optical conductivity (σ_{op}) is defined by [35]:

$$\sigma_{op} = \frac{\alpha n c}{4\pi} \quad (7)$$

where c - is the light velocity.

3. RESULTS AND DISCUSSION

3.1. Morphological and Structural Investigation

The surface morphology, illustrated in Fig. 2, of the PVA/PAA polymer blend doped with different concentrations (0, 0.6, 1.2) wt.% of SiC/MWCNTs. It is clear that the polymer blend was completely dissolved in the solution. Fig. 2 demonstrates that SiC/MWCNTs were evenly distributed on the polymer blend's surface.

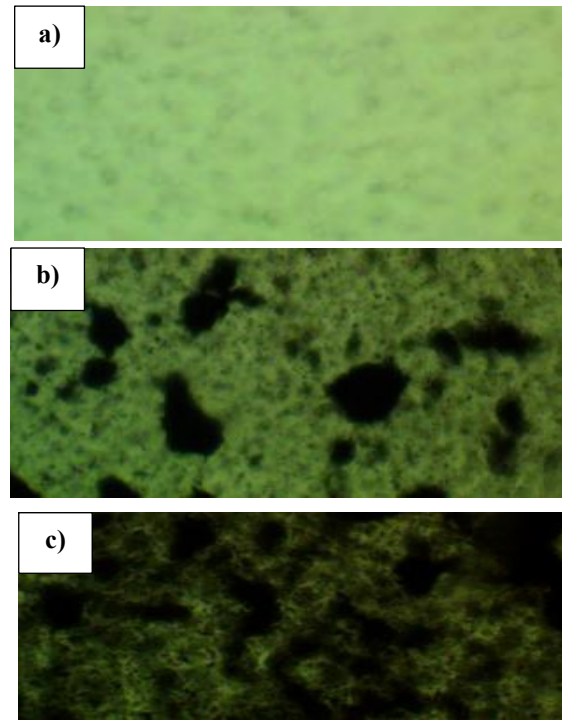


Fig. 2. Optical microscopy image at 100X for PVA/PAA polymer blend with different concentrations of SiC/MWCNTs: a) blend, b) 0.6% and c) 1.2%

At high SiC/MWCNT concentrations, a network of pathways is forming on the polymer blend's matrix, which is crucial for the mobility of charge carriers [36,37].

Fig. 3 illustrates the FE-SEM images of PVA/PAA doped with different concentrations of SiC/MWCNTs. Field emission electron microscopy has been used to study the compatibility of

PVA/PAA polymer blend with SiC/MWCNTs. The films have a uniform grain distribution at the surface morphology, while the surface of PVA/PAA-SiC/MWCNTs nanocomposites has many aggregates of nanoparticles randomly scattered in the polymer blend. The results show that as the ratio of SiC/MWCNTs increased, the number of aggregations on the polymer blend increased. Additionally, the FESEM demonstrates the formation of a network of pathways within the polymer blend matrix that allows charge carriers to move through it [38].

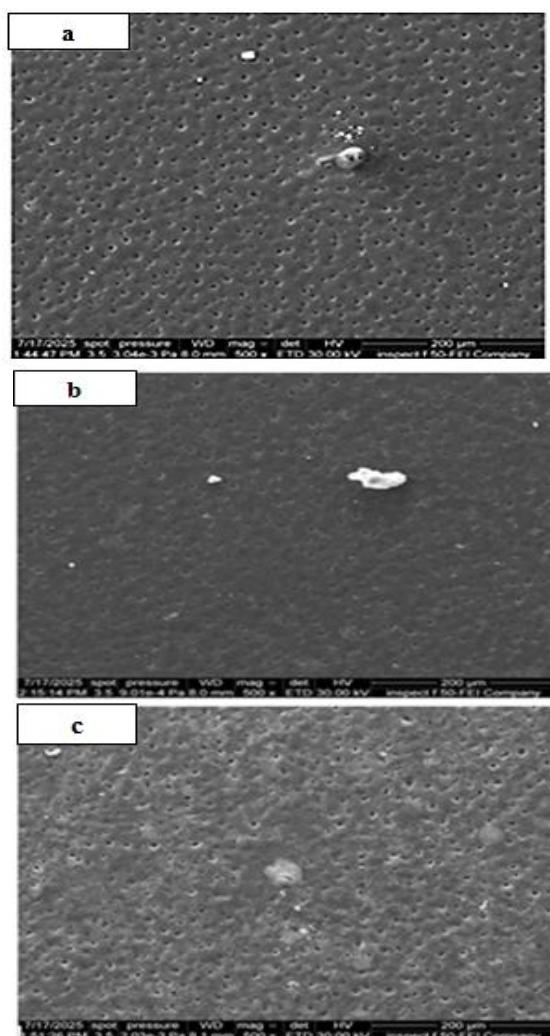
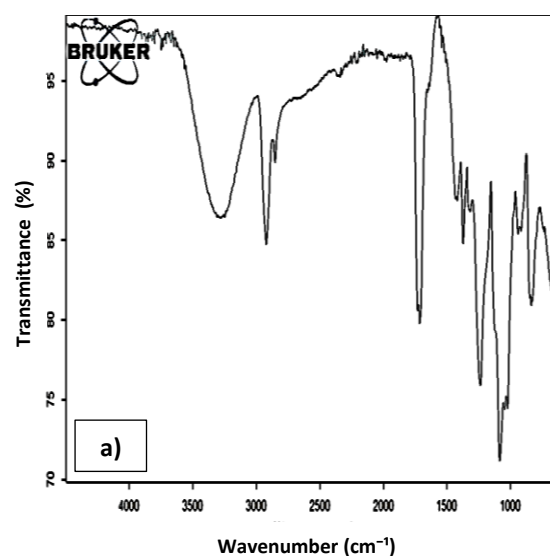


Fig. 3. FESEM image for PVA/PAA polymer blend with different concentrations of SiC/MWCNTs: a) blend, b) 0.6% and c) 1.2%

Fig. 4 illustrates the FTIR spectra of PVA/PAA polymer blend doped SiC/MWCNTs nanocomposites. It shows that PVA and PAA's distinctive absorption bands are visible in the blend spectrum because of intermolecular hydrogen bonds in both PVA and PAA; there is a broad O–H stretching band around 3200–3500 cm^{-1} . Stretching

C–H at about 2900 cm^{-1} . The presence of carboxylic acid groups from PAA is indicated by the C=O stretching vibration about 1700–1720 cm^{-1} . The normal range for C–O stretching and C–O–C vibrations is 1000–1300 cm^{-1} . Peaks corresponding to $-\text{CH}_2$ bending vibrations are located between 1430 and 1460 cm^{-1} . The transmittance in the fingerprint region (1000–1300 cm^{-1}) slightly decreases, suggesting dispersion of fillers that may interfere with polymer chain vibrations; the O–H band broadens or shifts slightly, suggesting stronger hydrogen bonding or interaction between the polymer matrix and the filler surface (hydroxyl groups interacting with MWCNTs or surface oxides on SiC); these changes imply interfacial interactions between the polymer chains and SiC/MWCNTs at low loading, potentially improving compatibility and dispersion. A slight shift or reduction in intensity may be seen in the C=O peak near 1700 cm^{-1} . With increased doping, because of filler agglomeration or bonding site saturation, the O–H band gets much broader and less strong, suggesting a more significant interaction or potential disruption of hydrogen bonding. Overall, peak intensities have significantly decreased, particularly in the 1000–1500 cm^{-1} range. This might be because of more filler that absorbs infrared light, decreased crystallinity or chain mobility as a result of adding filler, potential aggregation and increased dispersion [39–41].



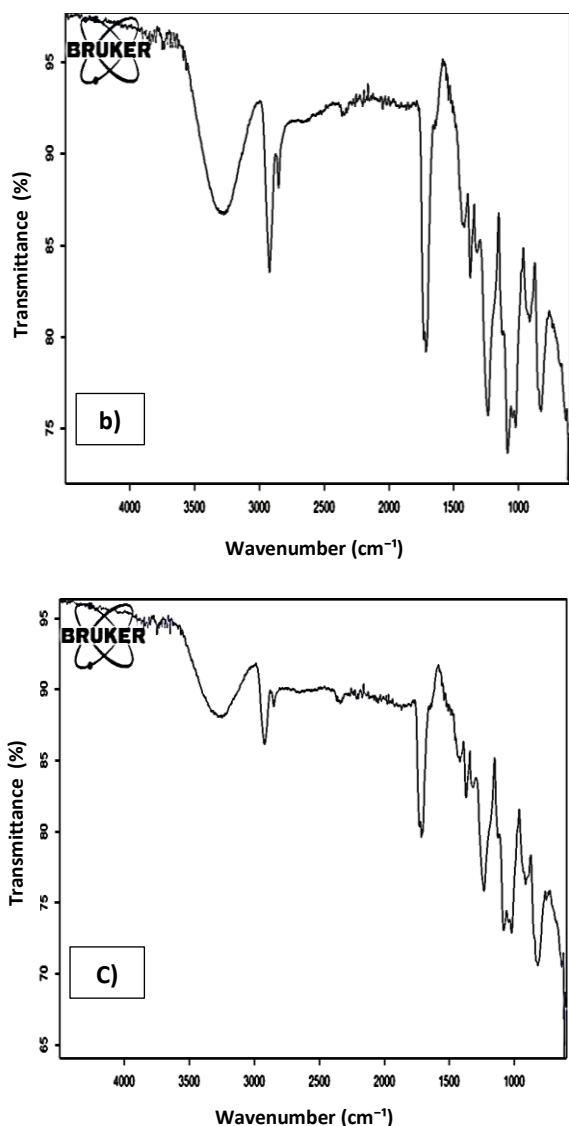


Fig. 4. FTIR spectra for PVA/PAA polymer blend with different concentrations of SiC/MWCNTs: a) blend, b) 0.6% and c) 1.2%

3.2. Optical Properties Investigation

In this section, the optical properties of PVA/PAA-SiC/MWCNTs are investigated and studied. Fig. 5 illustrates the variation of absorbance spectra of PVA/PAA polymer blend doped with SiC/MWCNTs against photon wavelength for different concentrations of SiC/MWCNTs. All the results showed a high absorbance peak in the ultraviolet, and its value becomes low at the visible region, which is related to the fact that doping the PVA/PAA polymer blend with SiC/MWCNTs enhances the absorption due to localized surface plasmon resonance (LSPR) and increased interfacial polarization. This amplifies UV absorption, particularly due to electron

delocalization and charge transfer between the polymer matrix and the nanofillers [42].

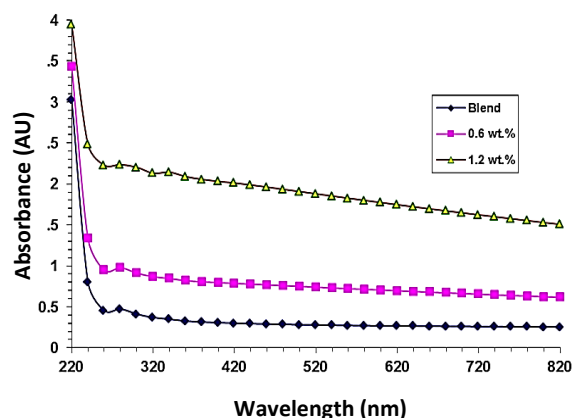


Fig. 5. The absorbance versus wavelength for PVA/PAA-SiC/MWCNTs films

Fig. 6 shows the transmittance of PVA/PAA doped SiC/MWCNTs versus the wavelength. As is obvious from Fig. 5, the transmittance increased with photon wavelength, but it decreased with increasing the content of SiC/MWCNTs. The increase in transmittance of PVA/PAA-doped SiC/MWCNT films with higher nanoparticle content is mainly due to improved nanoparticle dispersion, which reduces light scattering and enhances optical clarity. Additionally, better refractive index matching between the nanoparticles and the polymer matrix, as well as reduced surface roughness, contribute to higher light transmission. These effects are typically observed up to an optimal loading level, beyond which agglomeration may reverse the trend [43].

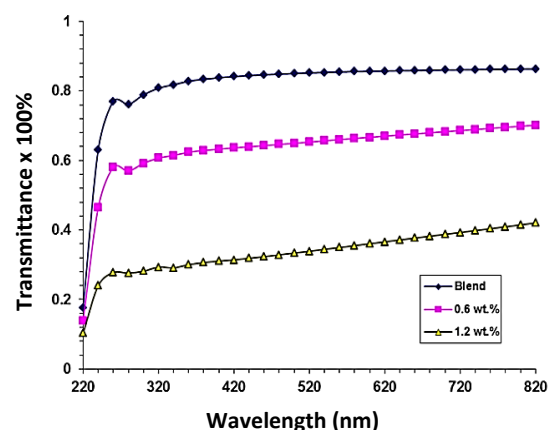


Fig. 6. The transmittance versus wavelength for PVA/PAA-SiC/MWCNTs films

Fig. 7 illustrates the absorption coefficient of the PVA/PAA polymer blend doped with SiC/MWCNTs, which gives information about the nature of the transition that occurs. It is observed that the $\alpha < 10^4 \text{ cm}^{-1}$; therefore, an indirect transition happened. The film's capacity to absorb photons is improved as the amount of SiC and MWCNT nanoparticles rises because more light-absorbing species are added to the PVA/PAA matrix. Because of their delocalized π -electron systems, MWCNTs in particular have substantial broadband absorption; SiC also contributes through its inherent optical characteristics. The overall absorption coefficient is raised by the combined effects of increased light-matter interaction and potential localized energy state creation [44].

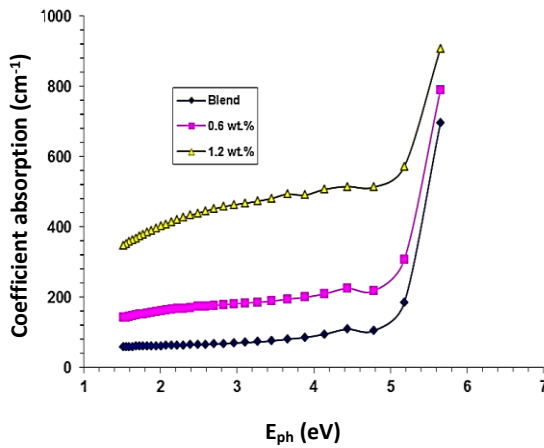


Fig.7. The absorption coefficient for PVA/PAA polymer blend with different concentrations of SiC/MWCNTS

The values of allowed and forbidden are illustrated in Figs. 8 and 9 respectively. The optical band gap narrows as the amount of SiC and MWCNT nanoparticles rises because they introduce defect states and localized energy levels into the polymer blend matrix [45]. As a result, the absorption edge shifts red, indicating a reduction in the allowed energy gaps from 4.8 eV to 3.82 eV and forbidden energy gaps.

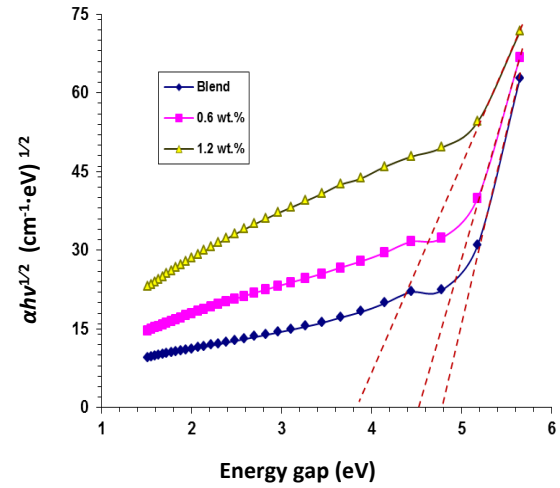


Fig. 8. Allowed energy gap values for PVA/PAA polymer blend with different concentrations of SiC/MWCNTS

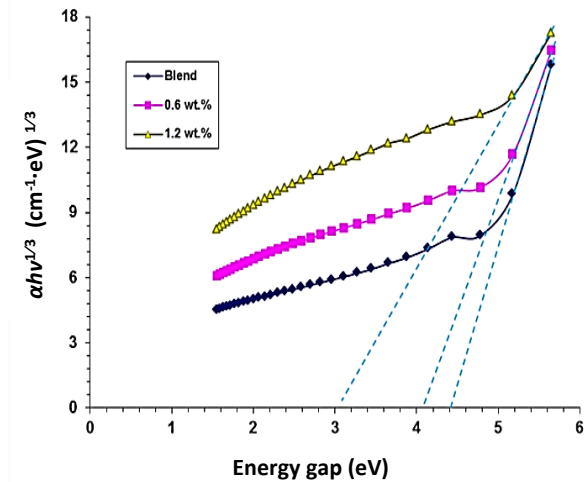


Fig. 9. Forbidden energy gap values for PVA/PAA-SiC/MWCNTS films

Figs. 10 and 11 illustrate the performance of n and k for PVA/PAA polymer blend doped SiC/MWCNTs. Both n and k increased with increasing the content of SiC/MWCNTs nanoparticles. The overall polarizability and optical density of the film increase with increasing SiC/MWCNT nanoparticle content, resulting in a higher refractive index n . Because of the greater light absorption by MWCNTs and the scattering from evenly distributed nanoparticles, the extinction coefficient k also rises. As nanoparticle loading rises, these effects suggest stronger light-matter interactions and increased photon attenuation [46].

The real ϵ_1 and imaginary ϵ_2 parts of the dielectric constant are illustrated in Figs. 12 and 13 both of ϵ_1 and ϵ_2 decreased with increasing the wavelength accept for last ratio of SiC/MWCNTs,

generally ε_1 and ε_2 increased with the content of NPs, The real part ε_1 of the dielectric constant increases as the SiC and MWCNT nanoparticle concentration in the PVA/PAA matrix increases because of the higher polarizability and density of electronic states, which improves the film's capacity to store electric field energy. Due to increased optical absorption and charge carrier loss, which are mainly caused by MWCNTs' conductive and absorptive properties, the imaginary part ε_2 also rises [47].

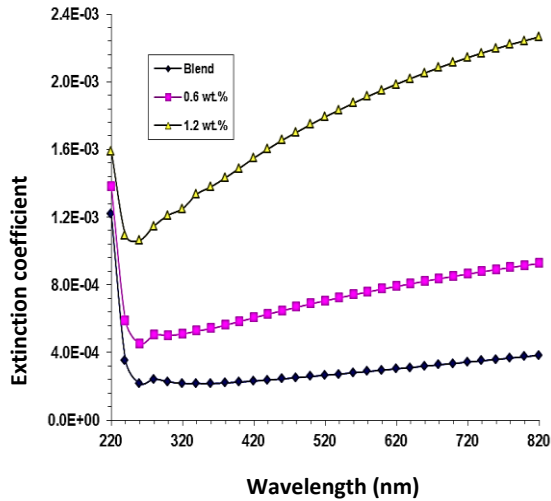


Fig. 10. Performance of k for PVA/PAA-SiC/MWCNTs films

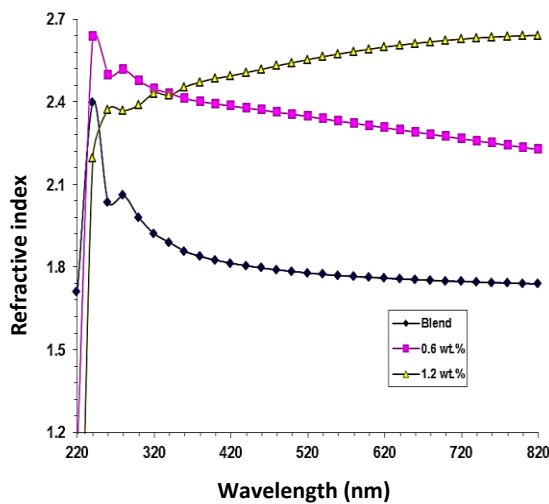


Fig. 11. Performance of n for PVA/PAA polymer blend doped SiC/MWCNTs

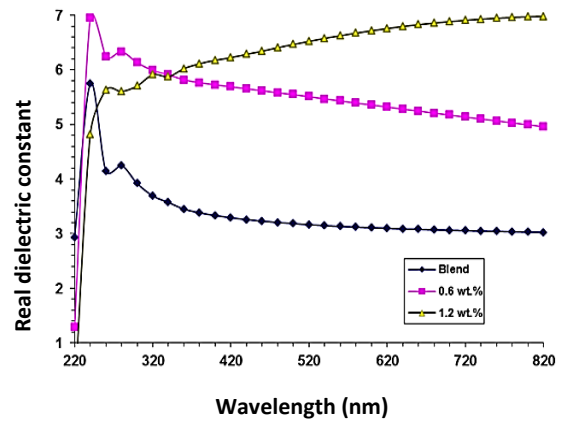


Fig. 12. ε_1 behavior for PVA/PAA polymer blend with different concentrations of SiC/MWCNTs

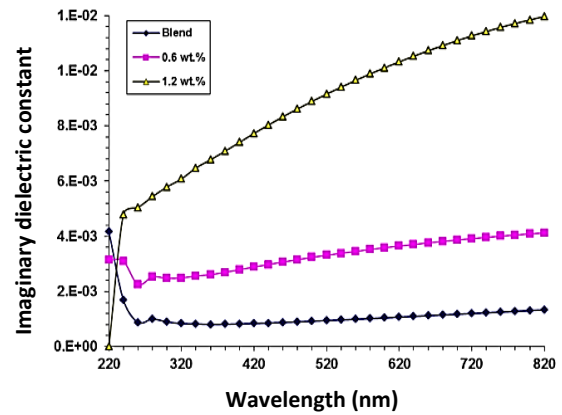


Fig. 13. ε_2 behavior for PVA/PAA polymer blend with different concentrations of SiC/MWCNTs

Fig. 14 shows the optical conductivity as a function of wavelength for PVA/PAA polymer blend doped SiC/MWCNTs. It decreased with increasing photon wavelength; generally, the optical conductivity increased with increasing the content of SiC/MWCNTs [48].

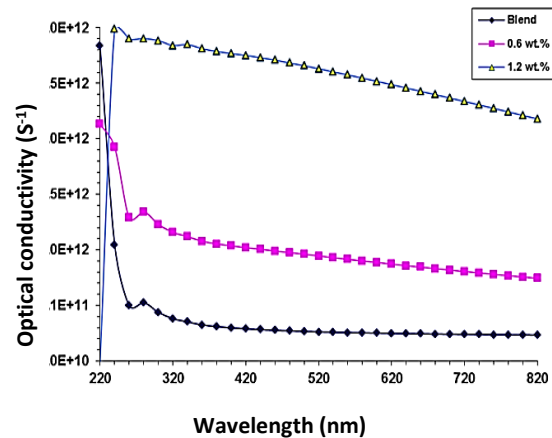


Fig. 14. Optical conductivity variation with wavelength for PVA/PAA polymer blend with different concentrations of SiC/MWCNTs

4. CONCLUSION

The PVA/PAA polymer blend dope SiC/MWCNTs nanocomposites were successfully prepared through the traditional casting method. The optical microscopy image shows that the polymer blend was well dispersed in the solution, and the NPs were well distributed on the polymer blend matrix. FESEM analysis shows that the films have a uniform grain distribution at the surface morphology of the polymer blend. The FTIR analysis indicates the absence of new functional groups in the prepared samples, which means that only a physical interaction has occurred. It was observed from the study of optical properties that the increase in SiC/MWCNTs NPs leads to enhancement of all optical features such as absorbance, refractive index, optical conductivity, real and imaginary part of dielectric constant, while transmittance and energy gap were decreased. The energy gap decreased from 4.8 eV to 3.82 eV for allowed transition and from 4 eV to 3.02 eV for forbidden transition. These results show that PVA/PAA-doped SiC/MWCNTs films can be utilized in advanced applications.

CONFLICTS OF INTEREST

The authors declare no conflict of interest.

REFERENCES

- [1] J. Amalraj, P. Lakshmanan, C.A. Amarnath, R.D. Pyarasani, C. Saravanan, Biodegradable polymer blend nanocomposites for energy storage application. *Polymer blend nanocomposites for energy storage applications*, 2023: 175–202. <https://doi.org/10.1016/B978-0-323-99549-8.00009-1>
- [2] J.-W. Li, C.-C. Cheng, C.-W. Chiu, Advances in Multifunctional Polymer-Based Nanocomposites. *Polymers*, 16(23), 2024: 3440. <https://doi.org/10.3390/polym16233440>
- [3] K. Asim, M. Khalid, W. Ullah, M. Younas, I. Boukhris, M.G.B. Ashiq, Structural, dielectric and magnetic properties of MWCNTs coated magnesium spinel ferrites nanocomposites. *Materials Research Bulletin*, 188, 2025: 113433. <https://doi.org/10.1016/j.materresbull.2025.113433>
- [4] X. Li, G. Zeng, X. Lei, The stability, optical properties and solar-thermal conversion performance of SiC-MWCNTs hybrid nanofluids for the direct absorption solar collector (DASC) application. *Solar Energy Materials and Solar Cells*, 206, 2020: 110323. <https://doi.org/10.1016/j.solmat.2019.110323>
- [5] J.-W. Li, C.-C. Cheng, C.-W. Chiu, Advances in Multifunctional Polymer-Based Nanocomposites. *Polymers*, 16(23), 2024: 3440. <https://doi.org/10.3390/polym16233440>
- [6] O. Agboola, O.S.I. Fayomi, A. Ayodeji, A.O. Ayeni, E.E. Alagbe, S.E. Sanni, E.E. Okoro, L. Moropeng, R. Sadiku, K.W. Kupolati, B.A. Oni, A Review on Polymer Nanocomposites and Their Effective Applications in Membranes and Adsorbents for Water Treatment and Gas Separation. *Membranes*, 11(2), 2021: 139. <https://doi.org/10.3390/membranes11020139>
- [7] Y. Cheng, Y. Hu, M. Xu, M. Qin, W. Lan, D. Huang, Y. Wei, W. Chen, High strength polyvinyl alcohol/polyacrylic acid (PVA/PAA) hydrogel fabricated by Cold-Drawn method for cartilage tissue substitutes. *Journal of Biomaterials Science, Polymer Edition*, 31(14), 2020: 1836–1851. <https://doi.org/10.1080/09205063.2020.1782023>
- [8] Liu, Z., Hu, Y., Gong, Y., Cheng, Y., Yang, H., Kang, M., Ding, H., Lei, Z., Wei, Y., & Huang, D. (2023). A facile method to fabricate high performance PVA/PAA-AS hydrogel via the synergy of multiple hydrogen bonding and Hofmeister effect. *Journal of Biomaterials Science, Polymer Edition*, 34(2), 243–257. <https://doi.org/10.1080/09205063.2022.2115759>
- [9] M.E. Diken, B. Koçer Kizilduman, B.Y. Kardaş, E.M. Doğan, M. Doğan, Y. Turhan, S. Doğan, Synthesis, characterization, and their some chemical and biological properties of PVA/PAA/nPS hydrogel nanocomposites: Hydrogel and wound dressing. *Journal of Bioactive and Compatible Polymers*, 35(3), 2020: 268–282. <https://doi.org/10.1177/0883911520921474>
- [10] M. Govender, S. Indermun, P. Kumar, Y.E. Choonara, V. Pillay, 3D printed, PVA–PAA hydrogel loaded-polycaprolactone scaffold for the delivery of hydrophilic in-situ formed sodium indomethacin. *Materials*, 11(6), 2018: 1006. <https://doi.org/10.3390/ma11061006>
- [11] D.A. Bichara, H. Bodugoz-Sentruk, D. Ling, E. Malchau, C.R. Bragdon, O.K. Muratoglu,

- Osteochondral defect repair using a polyvinyl alcohol-polyacrylic acid (PVA-PAAc) hydrogel. *Biomedical Materials*, 9(4), 2014: 045012. <https://doi.org/10.1088/1748-6041/9/4/045012>
- [12] Liang, X., Zhong, H. J., Ding, H., Yu, B., Ma, X., Liu, X., Chong, C. M., & He, J. (2024). Polyvinyl alcohol (PVA)-based hydrogels: Recent progress in fabrication, properties, and multifunctional applications. *Polymers*, 16(19), 2755. <https://doi.org/10.3390/polym16192755>
- [13] Q. Huang, C. Wan, M. Loveridge, R. Bhagat, Partially neutralized polyacrylic acid/poly(vinyl alcohol) blends as effective binders for high-performance silicon anodes in lithium-ion batteries. *ACS Applied Energy Materials*, 1(12), 2018: 6890–6898. <https://doi.org/10.1021/acsaem.8b01277>
- [14] P. Parikh, M. Sina, A. Banerjee, X. Wang, M.S. D'Souza, J.-M. Dour, E.A. Wu, O.Y. Trieu, Y. Gong, Q. Zhou, K. Snyder, Y.S. Meng, Role of polyacrylic acid (PAA) binder on the solid electrolyte interphase in silicon anodes. *Chemistry of Materials*, 31(7), 2019: 2535–2544. <https://doi.org/10.1021/acs.chemmater.8b05020>
- [15] H. Ahmed, A. Hashim, Tuning the Spectroscopic and Electronic Characteristics of ZnS/SiC Nanostructures Doped Organic Material for Optical and Nanoelectronics Fields. *Silicon*, 15, 2023: 2339–2348. <https://doi.org/10.1007/s12633-022-02173-w>
- [16] H.K. Jaafar, A. Hashim, B.H. Rabee, Fabrication and tuning the morphological and optical characteristics of PMMA/PEO/SiC/BaTiO₃ newly quaternary nanostructures for optical and quantum electronics fields. *Optical and Quantum Electronics*, 55, 2023: 989. <https://doi.org/10.1007/s11082-023-05208-7>
- [17] M. Nur-E-Alam, A Study on the Multifunctional Properties and Application Perspectives of ZnO/SiC Composite Materials. *Inorganics*, 13(7), 2025: 235. <https://doi.org/10.3390/inorganics13070235>
- [18] H.A.J. Hussien, A. Hashim, Fabrication and Analysis of PVA/TiC/SiC Hybrid Nanostructures for Nanoelectronics and Optics Applications. *Journal of Inorganic and Organometallic Polymers and Materials*, 34, 2024: 2716–2727. <https://doi.org/10.1007/s10904-024-03007-5>
- [19] N.A.-H. Al-Aaraji, A. Hashim, H.M. Abduljalil, A. Hadi, Tailoring the design, structure and spectroscopic characteristics of SiC/CuO doped transparent polymer for photonics and quantum nanoelectronics fields. *Optical and Quantum Electronics*, 55, 2023: 743. <https://doi.org/10.1007/s11082-023-05048-5>
- [20] F. Stergioudi, A. Prospathopoulos, A. Farazas, E.C. Tsirogiannis, N. Michailidis, Mechanical Properties of AA2024 Aluminum/MWCNTs Nanocomposites Produced Using Different Powder Metallurgy Methods. *Metals*, 12(8), 2022: 1315. <https://doi.org/10.3390/met12081315>
- [21] Y. Huang, J. Li, L. Wan, X. Meng, Y. Xie, Strengthening and toughening mechanisms of CNTs/Mg-6Zn composites via friction stir processing. *Materials Science and Engineering: A*, 732, 2018: 205–211. <https://doi.org/10.1016/j.msea.2018.07.011>
- [22] S.R. Bakshi, A. Agarwal, An analysis of the factors affecting strengthening in carbon nanotube reinforced aluminum composites. *Carbon*, 49, 2011: 533–544. <https://doi.org/10.1016/j.carbon.2010.09.054>
- [23] J.G. Park, D.H. Keum, Y.H. Lee, Strengthening mechanisms in carbon nanotube-reinforced aluminum composites. *Carbon*, 95, 2015: 690–698. <https://doi.org/10.1016/j.carbon.2015.08.112>
- [24] L. Jiang, G. Fan, Z. Li, X. Kai, D. Zhang, Z. Chen, S. Humphries, G. Heness, W.Y. Yeung, An approach to the uniform dispersion of a high volume fraction of carbon nanotubes in aluminum powder. *Carbon*, 49(6), 2011: 1965–1971. <https://doi.org/10.1016/j.carbon.2011.01.021>
- [25] Y. Zhang, X. Li, H. Chen, Synergistic effects of SiC and MWCNTs on the thermal and mechanical performance of polymer composites. *Composites Science and Technology*, 237, 2023: 110364. <https://doi.org/10.1016/j.compscitech.2023.110364>
- [26] A.A. Al-Muntaser, E. Alzahrani, G.M. Asnag, A.Y. Yassin, Tailoring Structural, Optical, and Dielectric Properties of PVC/PMMA/PS/ZnO Nanocomposites for Capacitive Energy Storage Applications. *ECS Journal of Solid State Science and Technology*, 14(3), 2025: 033001. <https://doi.org/10.1149/2162-8777/adb992>
- [27] A.A. Al-Muntaser, S.A. Al-Ghamdi, E. Alzahrani, A. Rajeh, G.M. Asnag, A.M. Al-Harthi, R. Alwafi, A. Saeed, S. Aldwais, A.Y. Yassin, Investigation of structural and optical characteristics of PVA/crystal violet dye composites for flexible

- smart optoelectronic applications. *Journal of Polymer Research*, 31, 2024: 311.
<https://doi.org/10.1007/s10965-024-04160-8>
- [28] A.A. Al-Muntaser, E. Alzahrani, A. Saeed, S.A. Al-Ghamdi, R. Alwafi, H.M. Abo-Dief, A.Y. Yassin, Exploring the influence of Sudan IV Azo dye on the structural, optical, and dispersion characteristics of PVA/Su-IV composites, *Physica Scripta*, 99(10), 2024: 10105991.
<https://doi.org/10.1088/1402-4896/ad79a2>
- [29] N.A. Kattan, E. Alzahrani, M.A. Morsi, G.M. Asnag, A.A. Al-Muntaser, S.H. Khoreem, A.Y. Yassin, Optimizing PEO/HPMC polymer blends with Al₂O₃/MoO₃ as hybrid nanofiller for enhanced dielectric performance and energy storage systems. *Reactive and Functional Polymers*, 216, 2025: 106432.
<https://doi.org/10.1016/j.reactfunctpolym.2025.106432>
- [30] A.A.A. Ahmed, A.M. Al-Hussam, A.M. Abdulwahab, A.N.A.A. Ahmed. The impact of sodium chloride as dopant on optical and electrical properties of polyvinyl alcohol. *AIMS Materials Science*, 5(3), 2018: 533-542.
<https://doi.org/10.3934/matersci.2018.3.533>
- [31] A.M.A. Henaish, A.S. Abouhaswa, Effect of WO₃ nanoparticle doping on the physical properties of PVC polymer. *Bulletin of Materials Science*, 43(1), 2020: 149.
<https://doi.org/10.1007/s12034-020-02109-3>
- [32] K. Mahalakshmi, V. Lakshmi, S.D.C. Anitha, R. MaryJenila, Optical, structural and morphological analysis of rGO decorated CoSe₂ nanocomposites. *International Journal of Innovative Science Engineering & Technology*, 8(2), 2021: 180-192.
https://ijiset.com/vol8/v8s2/IJISSET_V8_I02_16.pdf
- [33] G. Santhosh, G.P. Nayaka, B.S. Madhukar and Siddaramaiah, Optical properties of PVP/Li₃GaO₃ nanocomposites. *Materials Today: Proceedings*, 4, 2017: 12061-12069.
<https://doi.org/10.1016/j.matpr.2017.09.131>
- [34] P.O. Amin, K.A. Ketuly, S.R. Saeed, F.F. Muhammadsharif, M.D. Symes, A. Paul, K. Sulaiman, Synthesis, spectroscopic, electrochemical and photophysical properties of high band gap polymers for potential applications in semi-transparent solar cells. *BMC Chemistry*, 15, 2021: 25.
<https://doi.org/10.1186/s13065-021-00751-4>
- [35] A.O. Salohub, A.A. Voznyi, O.V. Klymov, N.V. Safryuk, D.I. Kurbatov, A.S. Opanasyuk. Determination of fundamental optical constants of Zn₂SnO₄ films. *Semiconductor Physics, Quantum Electronics & Optoelectronics*, 20(1), 2017: 79-84.
<https://doi.org/10.15407/spqeo20.01.079>
- [36] A. El-Sayed, S.H. El-Sabbagh, M.A. Abdelwahab, A.I. Abd El-Fattah, FTIR evidence of interfacial interaction in polymer/CNT nanocomposites. *Polymer Testing*, 124, 2023: 108031.
<https://doi.org/10.1016/j.polymertesting.2023.108031>
- [37] A. Hashim, A. Hadi, M.H. Abbas, Synthesis and Unraveling the Morphological and Optical Features of PVP-Si₃N₄-Al₂O₃ Nanostructures for Optical and Renewable Energies Fields. *Silicon*, 15, 2023: 6431–6438
<https://doi.org/10.1007/s12633-023-02529-w>
- [38] A. Kareem, A. Hashim, H.B. Hassan, Ameliorating and tailoring the morphological, structural, and dielectric features of Si₃N₄/CeO₂ futuristic nanocomposites doped PEO for nanoelectronic and nanodielectric applications. *Journal of Materials Science: Materials in Electronics*, 35, 2024: 461.
<https://doi.org/10.1007/s10854-024-12278-0>
- [39] M. H. Abdel-Kader, M.B. Mohamed, T. Alharby, R. M. Ibrahim, UV-irradiation effects on the structural, optical and electrical characteristics of soft blended polymeric materials loaded with multi-walled carbon nanotubes (MWCNTs). *Journal of Macromolecular Science, Part B*, 64(5), 2025: 531–554.
<https://doi.org/10.1080/00222348.2024.2357916>
- [40] S. Prakasam, N. Maharajan, G. Krishnan, S. Chinnathambi, Surface defect and composite effect triggered sensitivity enhancement in cobalt oxide-MWCNT nanostructure for electrochemical determination of chloramphenicol. *Microchemical Journal*, 216, 2025: 114705
<https://doi.org/10.1016/j.microc.2025.114705>
- [41] A. Hakamy, Investigation of double-layer capacitance, Warburg finite-length impedance and AC conductivity of PVA/MWCNT nanocomposite films for supercapacitor applications. *Journal of Power Sources*, 656, 2025: 238032.
<https://doi.org/10.1016/j.jpowsour.2025.238032>
- [42] P. Awandkar, S. Yawale, Exploring structural and optical properties of MWCNT @polymer based composites and implicating its application toward CO₂ gas detection at room

- temperature. *Ceramics International*. Advance online publication, 51(25), 2025: 45994-46010. <https://doi.org/10.1016/j.ceramint.2025.07.313>
- [43] Ravina, G. Srivastava, S. Kumar, N.K. Gautam, S. Dalela, M.A. Ahmad, A.M. Quraishi, P.A. Alvi, Exploration of optical, structural, and electrochemical properties of ZnO/MWCNTs nanocomposites for usage in supercapacitor. *Journal of Energy Storage*, 125, 2025: 116844. <https://doi.org/10.1016/j.est.2025.116844>
- [44] H.S. Alzahrani, A.I. Al-Sulami, Q.A. Alsulami, A. Rajeh, A systematic study of structural, conductivity, linear, and nonlinear optical properties of PEO/PVA-MWCNTs/ZnO nanocomposites films for optoelectronic applications. *Optical Materials*, 133, 2022: 112900. <https://doi.org/10.1016/j.optmat.2022.112900>
- [45] H.K. Jaafar, A. Hashim, B.H. Rabee, Synthesis and Boosting the Morphological and Optical Characteristics of SiC/SrTiO₃ Nanomaterials Doped PMMA/PEO for Tailored Optoelectronics Fields. *Silicon*, 16, 2024: 603–614. <https://doi.org/10.1007/s12633-023-02706-x>
- [46] A M.M. Ibrahim, A. Abou Elfadl, A.M. El Sayed, I.M. Ibrahim, Improving the optical, dielectric properties and antimicrobial activity of chitosan–PEO by GO/MWCNTs: Nanocomposites for energy storage and food packaging applications. *Polymer*, 267, 2023: 125650. <https://doi.org/10.1016/j.polymer.2022.125650>
- [47] M.V. Bindu, G.M. Joselin Herbert, Experimental investigation of stability, optical property and thermal conductivity of water based MWCNT-Al₂O₃-ZnO mono, binary and ternary nanofluid. *Synthetic Metals*, 287, 2022: 117058. <https://doi.org/10.1016/j.synthmet.2022.117058>
- [48] A.M. El Sayed, Synthesis, optical, thermal, electric properties and impedance spectroscopy studies on P(VC-MMA) of optimized thickness and reinforced with MWCNTs. *Results in Physics*, 17, 2020: 103025. <https://doi.org/10.1016/j.rinp.2020.103025>